Improved Model-Free Adaptive Load Frequency Control for Multi-Area Power Systems

Jiaoyuan Chen, Dawei Gong, Yuyang Zhao, Shijie Song and Minglei Zhu, *Member, IEEE*

***Abstract*—This brief proposes a novel improved model-free adaptive control (IMFAC) algorithm to address the load frequency control (LFC) problem in multi-area power systems. A new three-term criterion function is introduced and integrated into the traditional MFAC framework for the first time. By incorporating system state increments into the control input computation, the proposed algorithm enhances the suppression of overshoots and oscillations caused by frequency deviations due to sudden load changes. Moreover, the algorithm is entirely data-driven, eliminating the need for mathematical modeling of complex power system dynamics. The effectiveness of the proposed method is validated through theoretical analysis and simulation on a three-area power system.**

***Index Terms*—Data-driven control (DDC), load frequency control (LFC), model-free adaptive control (MFAC), multi-area power systems, three-term criterion function**

I. Introduction

LOAD frequency fluctuation is a common issue that affects the secure and stable operation of power systems [1], [2]. Severe fluctuations can degrade power supply quality in industrial applications, damage electrical equipment, and even cause failures in transmission lines and generator units. Therefore, load frequency control (LFC) remains a significant research topic in the field of power system control [2].

LFC first attracted attention and began to be studied in the 1950s [3]. Over the decades, various control theories have been applied to address LFC problems, including model predictive control [4], internal model control [5], and H_∞ control [6]. Although these methods are effective, they all rely on an accurate mathematical model of the power system. However, as the scale of modern power systems continues to grow, modeling becomes increasingly complex. Even when an accurate model is available, these methods can impose significant computational burdens.

Unlike model-based control methods, data-driven control (DDC) relies solely on the input-output data of the system, eliminating the need for a mathematical model. In the context of complex systems, data-driven control has been further advanced by incorporating event-triggered mechanisms, learning-based strategies, and a variety of other emerging techniques [7]–[9]. As a typical example of such systems, power systems have become a major application field for DDC [10]. Among DDC methods, PID control was first adopted as a simple approach to LFC problems [11], followed by various PID-based methods incorporating intelligent algorithms [12]. With the rise of neural network-based control, these methods have also been applied to LFC [13]. Model-free adaptive control (MFAC), as a prominent branch of DDC, has received considerable attention since its inception [14], [15]. In recent years, extensive research has focused on the theoretical development of MFAC including robust control and event-triggered control [16], [17]. Beyond theory, MFAC has been applied in various industrial scenarios, such as wind turbines [18], chemical process systems [19], and unmanned surface vessels [20]. Moreover, MFAC has also been applied to solve LFC problem [21]. However, since sudden load changes in power systems typically occur in a stepwise manner, the corresponding load frequency response can often be approximated by a step response. The traditional MFAC algorithm considers only the criteria of state error and control input variation. As a result, it tends to exhibit significant overshoot in response to such abrupt changes, leading to large and persistent oscillations.

Inspired by this, a novel improved model-free adaptive control (IMFAC) algorithm is proposed in this brief. The main contributions of this work are as follows:

1) This paper proposes a novel three-term IMFAC algorithm, which introduces a system state increment term into the criterion function of the traditional MFAC [14], [15], [21]. This enhancement improves the algorithm's ability to suppress sudden state changes and mitigate overshoots along with the resulting oscillations.
2) The stability of the proposed IMFAC algorithm, incorporating the new criterion function, is rigorously proven in the presence of bounded disturbances.
3) In contrast to the methods in [4]–[6], the proposed IMFAC algorithm relies solely on input-output data and does not require a mathematical model of the power system. This model-free nature enhances its adaptability to complex and large-scale power systems.

The remainder of this brief is organized as follows. Section II introduces the mathematical and data models of multi-area power systems. Section III develops the IMFAC algorithm and presents the corresponding stability analysis. Section IV provides simulation results to demonstrate the effectiveness of the proposed approach. Section V concludes the brief.

Jiaoyuan Chen, Dawei Gong and Yuyang Zhao are with University of Electronic Science and Technology of China, Chengdu 611731, China (e-mail: chen.jiaoyuan@std.uestc.edu.cn; pzhzhx@126.com; yuyangzhao1994@std.uestc.edu.cn). Shijie Song and Minglei Zhu are with Southwest Jiaotong University, Chengdu 611756, China (e-mail: shijie.song@swjtu.edu.cn; minglei.zhu@swjtu.edu.cn).

Dawei Gong is the corresponding author (e-mail: pzhzhx@126.com).

This is the accepted version of the following article: Jiaoyuan Chen, Dawei Gong*, Yuyang Zhao, Shijie Song and Minglei Zhu, "Improved Model-Free Adaptive Load Frequency Control for Multi-Area Power Systems," IEEE Transactions on Circuits and Systems II: Express Briefs, 2025. which has been published in final form at https://doi.org/10.1109/TCSII.2025.3598338.

II. Problem Formulation

A. Multi-Area Power System Modeling

In a multi-area power system, the mathematical model of the ith area is given by

$$\begin{cases} \Delta\dot{f}_i(t) = -\dfrac{D_i}{M_i}\Delta f_i(t) - \dfrac{1}{M_i}\Delta P_{tie-i}(t) \\ \qquad\qquad + \dfrac{1}{M_i}\big(\Delta P_{mi}(t) - \Delta P_{di}(t)\big) \\ \Delta\dot{P}_{mi}(t) = \dfrac{1}{T_{ti}}\big(P_{gi}(t) - P_{mi}(t)\big) \\ \Delta\dot{P}_{gi}(t) = \dfrac{1}{T_{gi}}\big(P_{ci}(t) - P_{gi}(t)\big) - \dfrac{1}{R_i T_{gi}}\Delta f_i(t) \\ \Delta\dot{P}_{tie-i}(t) = 2\pi\Big(\sum\limits_{j=1,j\neq i}^{N} T_{ij}\Delta f_i(t) - \sum\limits_{j=1,j\neq i}^{N} T_{ij}\Delta f_j(t)\Big) \end{cases}$$

where these parameters and symbols in (1) are defined as shown in Table I.

TABLE I
Definition of Parameters and Symbols

Symbol	Definition
ACE_i	Area control error (ACE) (p.u.)
ΔP_{mi}	Generator output power deviation (p.u.)
ΔP_{gi}	Governor valve position deviation (p.u.)
ΔP_{tie-i}	Tie line power deviation (p.u.)
Δf_i	Frequency deviation (Hz)
T_{ti}	Turbine time constants (s)
T_{gi}	Governor time constants (s)
D_i	Generator unit damping coefficient (p.u./Hz)
T_{ij}	Synchronizing torque coefficient of tie-line between two areas (p.u./Hz)
R_i	Speed droop (Hz/p.u.)
M_i	Inertia of generator (p.u.·s)

Given a sampling time T, the discrete-time model obtained using the zero-order hold (ZOH) method is as follows

$$\begin{cases} y_i(s+1) = G_i y_i(s) + H_i u_i(s) + W_i v_i(s) \\ \mathrm{ACE}_i(s+1) = C_i y_i(s+1) \end{cases} \tag{1}$$

where $s \in \mathbb{N}$ is the time index. Additionally,

$$G_i = e^{A_i T}, \quad H_i = \int_0^T e^{A_i t} B_i dt, \quad W_i = \int_0^T e^{A_i t} F_i dt$$

$$A_i = \begin{bmatrix} -\frac{D_i}{M_i} & -\frac{1}{M_i} & \frac{1}{M_i} & 0 \\ 2\pi \sum\limits_{j=1,j\neq i}^{N} T_{ij} & 0 & 0 & 0 \\ 0 & 0 & -\frac{1}{T_{ti}} & \frac{1}{T_{ti}} \\ -\frac{1}{R_i T_{gi}} & 0 & 0 & -\frac{1}{T_{gi}} \end{bmatrix}$$

$$B_i = \begin{bmatrix} 0 & 0 & 0 & \frac{1}{T_{gi}} \end{bmatrix}^T, \quad C_i = \begin{bmatrix} D_i + \frac{1}{R_i} & 1 & 0 & 0 \end{bmatrix}$$

$$F_i = \begin{bmatrix} -\frac{1}{M_i} & 0 & 0 & 0 \\ 0 & -2\pi & 0 & 0 \end{bmatrix}^T$$

where $y_i(s) = [\Delta f_i(s)\ \Delta P_{tie-i}(s)\ \Delta P_{mi}(s)\ \Delta P_{gi}(s)]^T$ and $u_i(s) = \Delta P_{ci}(s)$ are the system state and the control input, respectively, and $v_i(s) = [\Delta P_{di}(s)\ \sum_{j=1,j\neq i}^{N} T_{ij}\Delta f_i(s)]^T$ is the disturbance vector.

Let $\beta_i = D_i + 1/R_i$ denote the frequency bias factor, the ACE of ith area is defined as

$$\mathrm{ACE}_i(s) = \beta_i \Delta f_i(s) + P_{tie-i}(s) \tag{2}$$

In (1), the system model is formulated as a linear discrete-time model after ZOH discretizations, which is commonly adopted in LFC studies [21], one has

$$\mathrm{ACE}_i(s+1) = C_i G_i y_i(s) + C_i H_i u_i(s) + C_i W_i v_i(s) \tag{3}$$

Although the matrices A_i, B_i, C_i, F_i, G_i, H_i and W_i are used in the analytical modeling of ACE, they are not required for implementing the control algorithm. The $\mathrm{ACE}_i(s+1)$ will be rewritten in a more general form, independent of these matrices, as follows

$$\mathrm{ACE}_i(s+1) = f_i(\mathrm{ACE}_i(s), u_i(s)) + \omega_i(s) \tag{4}$$

where $f_i(\cdot)$ is the unknown system function of the power system in ith area, $\omega_i(s) = C_i W_i v_i(s)$ is bounded disturbance and system (4) adheres to the two assumptions outlined below.

Assumption 1: Except for a finite set of time instants s, the partial derivatives of $f_i(\cdot)$ with respect to $u_i(s)$ remain continuous.

Assumption 2: System (4) is generalized *Lipschitz* continuous, that is, $\forall s_1 \neq s_2$, $s_1, s_2 \geq 0$ and $|u_i(s_1) - u_i(s_2)| \neq 0$, one has $|\mathrm{ACE}_i(s_1+1) - \mathrm{ACE}_i(s_2+1)| \leq q|u_i(s_1) - u_i(s_2)|$, where $q > 0$ is a positive constant.

B. Equivalent CFDL-Based Data Model for Multi-Area Power System

Lemma 1 ([21]): For the system (4) that satisfies Assumptions 1 and 2, when $|\Delta u_i(s)| = |u_i(s) - u_i(s-1)| \neq 0$, there must exist a perturbation parameter $\phi_i(s)$, referred to as the pseudo-partial derivative (PPD), enabling the transformation of system (4) into a CFDL-based data model.

$$\mathrm{ACE}_i(s+1) = \mathrm{ACE}_i(s) + \phi_i(s)\Delta u_i(s) + \Delta\omega_i(s) \tag{5}$$

where $\Delta\omega_i(s) = \omega_i(s) - \omega_i(s-1)$ and for any time s, $|\phi_i(s)|$ is bounded.

The data model (5) does not have a direct physical interpretation, it simply characterizes the relationship between input and output. Even in a linear time-invariant (LTI) system, the parameter $\phi_i(s)$, which represents the parameter perturbation dynamics (PPD), can vary over time. When the input $u_i(s)$ satisfies $|\Delta u_i(s)| \neq 0$ and the magnitude of the change $\Delta u_i(s)$ is not excessively large, $\phi_i(s)$ can be reasonably approximated as a slowly varying parameter.

III. Main Result

A. Design of IMFAC Algorithm

The criterion function for the control input is defined as follows

$$\begin{aligned} Q(u_i(s)) = {} & |\mathrm{ACE}_i^*(s+1) - \mathrm{ACE}_i(s+1)|^2 \\ & + \chi_i|\mathrm{ACE}_i(s+1) - \mathrm{ACE}_i(s)|^2 \\ & + \lambda_i|u_i(s) - u_i(s-1)|^2 \end{aligned} \tag{6}$$

where $\lambda_i, \chi_i > 0$ are two weight factors.

By substituting (5) into (6) and setting the derivative with respect to $u_i(s)$ to zero, we obtain

$$u_i(s) = u_i(s-1) + \rho_i \hat{\phi}_i(s) \frac{\mathrm{ACE}_i^*(s+1) - \mathrm{ACE}_i(s)}{\lambda_i + (1+\chi_i)|\hat{\phi}_i(s)|^2}$$

where $\hat{\phi}_i(s)$ is the estimation value of $\phi_i(s)$ and $0 < \rho_i \leq 1$ is a weight factor which makes the algorithm more flexible.

Remark 1: Compared to the traditional two-term criterion function in [14], [15], [21], the criterion function (6) adds an additional incremental term of ACE_i, enabling its rate of change to be incorporated into the calculation. This modification not only improves overshoot suppression but also provides explicit control over the response behavior via χ_i.

To implement the control algorithm, prior knowledge of the PPD value is required. Therefore, an estimation algorithm for PPD has been developed, with the criterion function given as

$$\begin{aligned} Q(\phi_i(s)) =& |\Delta \mathrm{ACE}_i(s) - \phi_i(s)\Delta u_i(s-1)|^2 \\ &+ \mu_i |\phi_i(s) - \hat{\phi}_i(s-1)|^2 \end{aligned} \tag{7}$$

where $\Delta \mathrm{ACE}_i(s) = \mathrm{ACE}_i(s) - \mathrm{ACE}_i(s-1)$ and $\mu_i > 0$ is a weight factor.

Using the modified projection algorithm, the unknown PPD is estimate to be

$$\begin{aligned} \hat{\phi}_i(s) =& \hat{\phi}_i(s-1) + \frac{\eta_i \Delta u_i(s-1)}{\mu_i + \Delta u_i(s-1)^2} \\ &\times \left(\Delta \mathrm{ACE}_i(s) - \hat{\phi}_i(s-1)\Delta u_i(s-1)\right) \end{aligned}$$

where $0 < \eta_i \leq 1$ is a weight factor which makes the algorithm more flexible. To enhance the predicting capability of PPD, the reset algorithm of $\hat{\phi}_i(s)$ is designed as follow

$$\hat{\phi}_i(s) = \hat{\phi}_i(1), \text{if } |\hat{\phi}_i(s)| \leq \varepsilon, \text{or } |\Delta u_i(s-1)| \leq \varepsilon$$

where ε is a small positive constant. The reset algorithm prevents stagnation and instability in PPD estimation under low excitation or near-zero estimates by re-initializing from a known feasible value, thereby enhancing predicting capability.

In order to ensure the stability of the load frequency, the desired ACE signal is designed to be $\mathrm{ACE}_i^*(s+1) = \mathrm{ACE}_i^*(s) = \mathrm{ACE}^* = 0$. Then, the IMFAC algorithm for ith area is developed as follows

$$\begin{aligned} \hat{\phi}_i(s) =& \hat{\phi}_i(s-1) + \frac{\eta_i \Delta u_i(s-1)}{\mu_i + \Delta u_i(s-1)^2} \\ &\times \left(\Delta \mathrm{ACE}_i(s) - \hat{\phi}_i(s-1)\Delta u_i(s-1)\right) \end{aligned} \tag{8}$$

$$\hat{\phi}_i(s) = \hat{\phi}_i(1), \text{if } |\hat{\phi}_i(s)| \leq \varepsilon, \text{or } |\Delta u_i(s-1)| \leq \varepsilon \tag{9}$$

$$u_i(s) = u_i(s-1) + \rho_i \hat{\phi}_i(s) \frac{\mathrm{ACE}^* - \mathrm{ACE}_i(s)}{\lambda_i + (1+\chi_i)|\hat{\phi}_i(s)|^2} \tag{10}$$

B. Stability Analysis

Before investigating the stabilization of the IMFAC algorithm, the following assumption is introduced.

Assumption 3: At any time instant s with $\Delta u_i(s) \neq 0$, the sign of $\phi_i(s)$ remains consistent; specifically, either $\phi_i(s) > \bar{b} > 0$ or $\phi_i(s) < -\bar{b}$, where $\bar{b}$ denotes a small positive constant. Without losing generality, this paper assumes that $\phi_i(s) > \bar{b} > 0$.

Assumption 3 essentially means that as control inputs increase, the corresponding outputs should remain non-decreasing, reflecting a "near-linear" behavior of the system (4). This assumption is similar to the invariant control direction assumed in model-based methods.

Theorem 1: The multi-area power systems (4), satisfying Assumptions 1,2 and 3. If the controller parameters are appropriately chosen, then, the following two conclusions hold.

1) The estimate value $\hat{\phi}_i(s)$ is boundedness.
2) The tracking errors $\zeta_i(s+1) = \mathrm{ACE}^* - \mathrm{ACE}_i(s+1)$ is convergent, with the final upper bound influenced by $|\Delta\omega_i(s+1)|$.

Proof: Define $\tilde{\phi}_i(s)$ as the PPD estimation error, $\tilde{\phi}_i(s) = \hat{\phi}_i(s) - \phi_i(s)$.

$$\begin{aligned} \tilde{\phi}_i(s) =& \tilde{\phi}_i(s-1) - \Delta\phi_i(s) + \frac{\eta_i \Delta u_i(s-1)}{\mu_i + \Delta u_i(s-1)^2} \\ &\times \left(\Delta \mathrm{ACE}_i(s) - \hat{\phi}_i(s-1)\Delta u_i(s-1)\right) \end{aligned} \tag{11}$$

where $\Delta\phi_i(s) = \phi_i(s) - \phi_i(s-1)$ denotes its increment.

Consequently, (11) equals to

$$\begin{aligned} \tilde{\phi}_i(s) =& \left(1 - \frac{\eta_i \Delta u_i(s-1)^2}{\mu_i + \Delta u_i(s-1)^2}\right)\tilde{\phi}_i(s-1) \\ &+ \frac{\eta_i \Delta u_i(s-1)}{\mu_i + \Delta u_i(s-1)^2}\Delta\omega_i(s-1) - \Delta\phi_i(s) \end{aligned} \tag{12}$$

According to the Lemma 1, one has that $|\phi_i(s)| \leq b_i$. Then, (12) becomes

$$\begin{aligned} |\tilde{\phi}_i(s)| \leq& \left|1 - \frac{\eta_i \Delta u_i(s-1)^2}{\mu_i + \Delta u_i(s-1)^2}\right| |\tilde{\phi}_i(s-1)| \\ &+ \left|\frac{\eta_i \Delta u_i(s-1)}{\mu_i + \Delta u_i(s-1)^2}\right| |\Delta\omega_i(s-1)| + 2b_i \end{aligned} \tag{13}$$

When $0 < \eta_i < 1, \mu_i > 0$, then $\eta_i \Delta u_i^2(s-1) \leq \Delta u_i^2(s-1) \leq \mu_i + \Delta u_i^2(s-1)$. Hence, $0 < \vartheta_i \leq \eta_i \Delta u_i(s-1)^2/(\mu_i + \Delta u_i(s-1)^2) < 1$, one can obtain that

$$\begin{aligned} \left|\frac{\eta_i \Delta u_i(s-1)}{\mu_i + \Delta u_i(s-1)^2}\right| =& \frac{\eta_i |\Delta u_i(s-1)|}{\mu_i + \Delta u_i(s-1)^2} \\ =& \frac{\eta_i}{\frac{\mu_i}{|\Delta u_i(s-1)|} + |\Delta u_i(s-1)|} \\ \leq& \frac{\eta_i}{2\sqrt{\mu_i}} \end{aligned} \tag{14}$$

Since $\omega_i(s)$ is bounded and δ_{ω_i} is the upper boundedness of $|\omega_i(s)|$. Define $\gamma_i = 2b_i + (\eta_i \delta_{\omega_i}/\sqrt{\mu_i})$, one has

$$\begin{aligned} |\tilde{\phi}_i(s)| &\leq (1-\vartheta_i)|\tilde{\phi}_i(s-1)| + \gamma_i \\ &\leq (1-\vartheta_i)^2 |\tilde{\phi}_i(s-2)| + \gamma_i(1-\vartheta_i) + \gamma_i \\ &\leq \cdots \\ &\leq (1-\vartheta_i)^{s-1} |\tilde{\phi}_i(1)| + \frac{\gamma_i}{\vartheta_i} \end{aligned} \tag{15}$$

which indicates the boundedness of $\tilde{\phi}_i(s)$. In conjunction with the boundedness of $\phi_i(s)$, it follows that $\hat{\phi}_i(s)$ is also bounded.

Considering the bounded disturbances $\omega_i(s)$, (10) is rewritten as

$$u_i(s) = u_i(s-1) + \rho_i \hat{\phi}_i(s) \frac{\zeta_i(s)}{\lambda_i + (1+\chi_i)|\hat{\phi}_i(s)|^2} \tag{16}$$

Let $\Gamma_i(s) = (\rho_i \phi_i(s)\hat{\phi}_i(s))/(\lambda_i + (1+\chi_i)|\hat{\phi}_i(s)|^2)$, we have

$$\zeta_i(s+1) = (1-\Gamma_i(s))\zeta_i(s) - \Delta\omega_i(s) \tag{17}$$

According to Assumption 3 and (9) we have $\phi_i(s)\hat{\phi}_i(s) \geq 0$, then

$$\begin{aligned}\Gamma_i(s) &= \frac{\rho_i \phi_i(s)\hat{\phi}_i(s)}{\lambda_i + (1+\chi_i)|\hat{\phi}_i(s)|^2} \leq \frac{b_i \hat{\phi}_i(s)}{\lambda_i + (1+\chi_i)|\hat{\phi}_i(s)|^2} \\ &\leq \frac{b_i \hat{\phi}_i(s)}{2\sqrt{\lambda_i(1+\chi_i)}\hat{\phi}_i(s)} \leq \frac{b_i}{2\sqrt{\lambda_i(1+\chi_i)}}\end{aligned} \tag{18}$$

From Assumption 3 and the parameter domain, it can be seen that $\Gamma_i(s) > 0$, when λ_i and χ_i take the suitable values, such that inequality $2\sqrt{\lambda_i(1+\chi_i)} > b_i$ holds, there exists a constant $0 < \Xi < 1$, one has

$$0 < \Xi < \frac{\rho_i \phi_i(s)\hat{\phi}_i(s)}{\lambda_i + (1+\chi_i)|\hat{\phi}_i(s)|^2} < 1 \tag{19}$$

Then, taking the absolute value of both sides of (17) gives

$$\begin{aligned}|\zeta_i(s+1)| &\leq |1-\Gamma_i(s)||\zeta_i(s)| + |\Delta\omega_i(s)| \\ &\leq (1-\Xi)^2|\zeta_i(s-1)| + 2(1-\Xi)\delta_{\omega_i} + 2\delta_{\omega_i} \\ &\vdots \\ &\leq (1-\Xi)^s|\zeta_i(1)| + \frac{2\delta_{\omega_i}}{\Xi}\end{aligned} \tag{20}$$

It is obvious that $\zeta_i(s+1)$ is bounded.

In summary, under Assumptions 1, 2, 3 and suitable parameter design, the proposed IMFAC algorithm guarantees boundedness of the PPD estimate and convergence of the tracking error, thereby ensuring closed-loop stability. ■

IV. Simulation Results

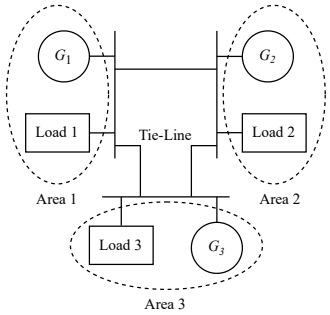

Fig. 1. Three-area power system.

As shown in Fig. 1, a three-area power system is considered in this section. The parameters of the power system in the three areas are listed as follows

1) Area 1

$$T_{t1} = 0.40 \text{ s},\ T_{g1} = 0.08 \text{ s},\ D_1 = 0.015 \text{ p.u./Hz}$$
$$M_1 = 0.1667 \text{ p.u.} \cdot \text{s},\ R_1 = 3 \text{ Hz/p.u.}$$

2) Area 2

$$T_{t2} = 0.44 \text{ s},\ T_{g2} = 0.06 \text{ s},\ D_2 = 0.016 \text{ p.u./Hz}$$
$$M_2 = 0.2017 \text{ p.u.} \cdot \text{s},\ R_2 = 2.73 \text{ Hz/p.u.}$$

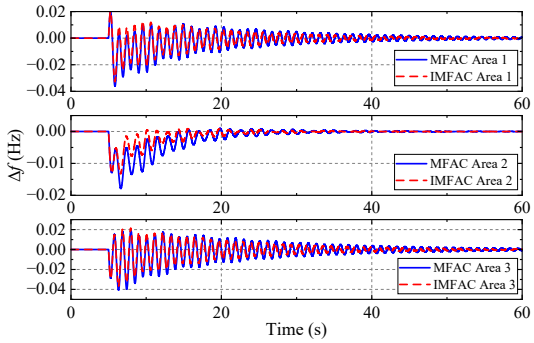

Fig. 2. The system state Δf_i in three areas.

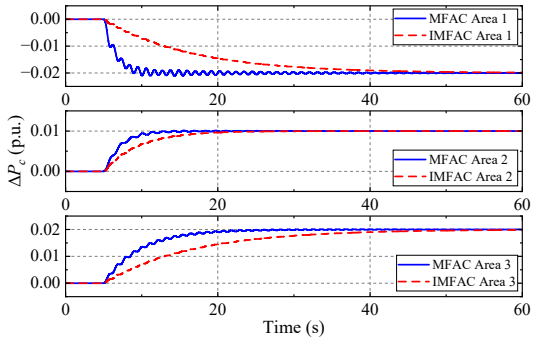

Fig. 3. The control input ΔP_{ci} in three areas.

3) Area 3

$$T_{t3} = 0.30 \text{ s},\ T_{g3} = 0.07 \text{ s},\ D_3 = 0.015 \text{ p.u./Hz}$$
$$M_3 = 0.1247 \text{ p.u.} \cdot \text{s},\ R_3 = 2.82 \text{ Hz/p.u.}$$

Synchronizing torque coefficient of tie-line between two areas are $T_{12} = T_{21} = 0.20$ p.u./Hz, $T_{13} = T_{31} = 0.25$ p.u./Hz, $T_{23} = T_{32} = 0.12$ p.u./Hz.

In the simulation, different magnitudes of load disturbances are applied at 5s to the power system in the three areas. The disturbances are set to -0.02 p.u., 0.01 p.u., and 0.02 p.u. for Areas 1, 2, and 3, respectively. The proposed IMFAC algorithm is employed to regulate the frequency deviation and is compared with the traditional MFAC algorithm [21]. The control parameters are as follows: Area 1: $\rho_1 = 0.01, \mu_1 = 1.4, \eta_1 = 0.3, \lambda_1 = 5, \chi_1 = 400, \epsilon_1 = 10^{-5}$; Area 2: $\rho_2 = 0.01, \mu_2 = 1.2, \eta_2 = 0.5, \lambda_2 = 5, \chi_2 = 10, \epsilon_2 = 10^{-5}$; Area 3: $\rho_3 = 0.01, \mu_3 = 1.3, \eta_3 = 0.5, \lambda_3 = 5, \chi_3 = 400, \epsilon_3 = 10^{-5}$. Fig. 2 and 3 plots the system state Δf and the control input ΔP_c, respectively. Fig. 4 shows the response of ΔP_{tie}. Fig. 5 compares the performance of sliding mode control (SMC), fuzzy-PID, MFAC and IMFAC in regulating the frequency deviation of area 2.

Table II compares the performance of SMC, fuzzy-PID, traditional MFAC [21] and the proposed algorithm using four performance criteria: integral squared error (ISE,$\sum_{s=t_0}^{t_{end}} |\zeta(s)|^2$), integral absolute error (IAE,$\sum_{s=t_0}^{t_{end}} |\zeta(s)|$), integral time-weighted squared error (ITSE,$\sum_{s=t_0}^{t_{end}} s|\zeta(s)|^2$), and integral time-weighted absolute error (ITAE,$\sum_{s=t_0}^{t_{end}} s|\zeta(s)|$).

Through Fig.5 and Table II, it can be observed that when the power system experiences load disturbances, the proposed IM-

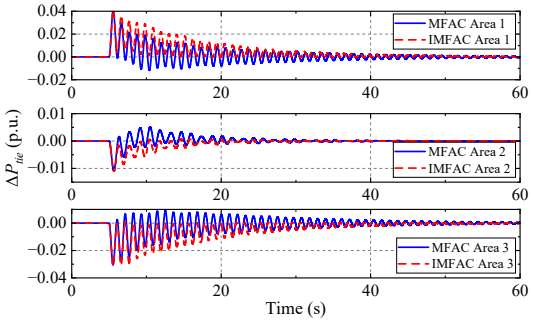

Fig. 4. Response of ΔP_{tie} in three areas.

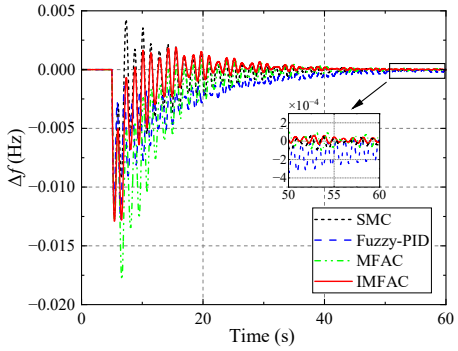

Fig. 5. Response of Δf_i in area 2.

TABLE II
PERFORMANCE COMPARISON

Algorithm	ISE	IAE	ITSE	ITAE
SMC	5.94	534.84	69.95	9.20e+03
Fuzzy-PID	5.76	648.17	90.41	1.27e+04
MFAC [21]	7.63	639.05	92.93	1.18e+04
IMFAC (our method)	**5.12**	**483.36**	**57.34**	**8.18e+03**

FAC algorithm effectively suppresses overshoot and achieves faster and smoother stabilization of the load frequency deviation. These results clearly demonstrate the superior regulation capability and dynamic performance of the proposed method in addressing multi-area load frequency control problems, especially in comparison to conventional approaches.

V. CONCLUSIONS

This brief proposes a novel IMFAC algorithm for LFC in multi-area power systems within a data-driven framework. By introducing a three-term criterion involving state increments, IMFAC effectively suppresses overshoot and oscillations caused by sudden load changes, without relying on system models. Simulations on a three-area system demonstrate its superior performance compared to traditional MFAC and other model-free methods. The proposed IMFAC framework exhibits flexibility for future extensions to address nonlinearities such as time delay, governor dead band, and generation rate constraints, as well as applications to modern power systems consisting of renewable energy integration.

REFERENCES

[1] H. H. Alhelou, M.-E. Hamedani-Golshan, R. Zamani, E. Heydarian-Forushani, and P. Siano, "Challenges and opportunities of load frequency control in conventional, modern and future smart power systems: a comprehensive review," *Energies*, vol. 11, no. 10, p. 2497, 2018.

[2] M. M. Gulzar, D. Sibtain, M. Alqahtani, F. Alismail, and M. Khalid, "Load frequency control progress: A comprehensive review on recent development and challenges of modern power systems," *Energy Strategy Reviews*, vol. 57, p. 101604, 2025.

[3] C. Concordia and L. Kirchmayer, "Tie-line power and frequency control of electric power systems [includes discussion]," *Transactions of the American Institute of Electrical Engineers. Part III: Power Apparatus and Systems*, vol. 72, no. 3, pp. 562–572, 1953.

[4] P. Ojaghi and M. Rahmani, "Lmi-based robust predictive load frequency control for power systems with communication delays," *IEEE Transactions on Power Systems*, vol. 32, no. 5, pp. 4091–4100, 2017.

[5] S. Saxena and Y. V. Hote, "Load frequency control in power systems via internal model control scheme and model-order reduction," *IEEE transactions on power systems*, vol. 28, no. 3, pp. 2749–2757, 2013.

[6] H. Zhang, J. Liu, and S. Xu, "H_∞ load frequency control of networked power systems via an event-triggered scheme," *IEEE Transactions on Industrial Electronics*, vol. 67, no. 8, pp. 7104–7113, 2019.

[7] M. Shen, X. Wang, S. Zhu, Z. Wu, and T. Huang, "Data-driven event-triggered adaptive dynamic programming control for nonlinear systems with input saturation," *IEEE Transactions on Cybernetics*, vol. 54, no. 2, pp. 1178–1188, 2023.

[8] Y. Jiang, D. Shi, J. Fan, T. Chai, and T. Chen, "Set-valued feedback control and its application to event-triggered sampled-data systems," *IEEE Transactions on Automatic Control*, vol. 65, no. 11, pp. 4965–4972, November 2020.

[9] M. Shen, X. Wang, J. H. Park, Y. Yi, and W.-W. Che, "Extended disturbance-observer-based data-driven control of networked nonlinear systems with event-triggered output," *IEEE Transactions on Systems, Man, and Cybernetics: Systems*, vol. 53, no. 5, pp. 3129–3140, 2022.

[10] G. Baggio, D. S. Bassett, and F. Pasqualetti, "Data-driven control of complex networks," *Nature communications*, vol. 12, no. 1, p. 1429, 2021.

[11] A. Khodabakhshian and N. Golbon, "Design of a new load frequency pid controller using qft," in *Proceedings of the 2005 IEEE International Symposium on, Mediterrean Conference on Control and Automation Intelligent Control, 2005.* IEEE, 2005, pp. 970–975.

[12] R. Dash, K. J. Reddy, B. Mohapatra, M. Bajaj, and I. Zaitsev, "An approach for load frequency control enhancement in two-area hydro-wind power systems using lstm+ ga-pid controller with augmented lagrangian methods," *Scientific Reports*, vol. 15, no. 1, p. 1307, 2025.

[13] S. D. Al-Majidi, M. Kh. AL-Nussairi, A. J. Mohammed, A. M. Dakhil, M. F. Abbod, and H. S. Al-Raweshidy, "Design of a load frequency controller based on an optimal neural network," *Energies*, vol. 15, no. 17, p. 6223, 2022.

[14] Z. Hou and W. Huang, "The model-free learning adaptive control of a class of siso nonlinear systems," in *Proceedings of the 1997 American control conference*, vol. 1. IEEE, 1997, pp. 343–344.

[15] Z. Hou and S. Jin, "A novel data-driven control approach for a class of discrete-time nonlinear systems," *IEEE Transactions on Control Systems Technology*, vol. 19, no. 6, pp. 1549–1558, 2010.

[16] M. Heydari, A. B. Novinzadeh, and M. Tayefi, "Anti wind-up and robust data-driven model-free adaptive control for mimo nonlinear discrete-time systems," *International Journal of Adaptive Control and Signal Processing*, 2024.

[17] B. Yue, M. Su, X. Jin, and W. Che, "Event-triggered mfac of nonlinear ncss against sensor faults and dos attacks," *IEEE Transactions on Circuits and Systems II: Express Briefs*, vol. 69, no. 11, pp. 4409–4413, 2022.

[18] M. Corradini, G. Ippoliti, G. Orlando, and D. Corona, "A data-driven model-free adaptive controller with application to wind turbines," *ISA transactions*, vol. 136, pp. 267–274, 2023.

[19] S. Gao, D. Zhao, X. Yan, and S. K. Spurgeon, "Model-free adaptive state feedback control for a class of nonlinear systems," *IEEE Transactions on Automation Science and Engineering*, vol. 21, no. 2, pp. 1824–1836, 2023.

[20] Y. Wang, C. Shen, J. Huang, and H. Chen, "Model-free adaptive control for unmanned surface vessels: A literature review," *Systems Science & Control Engineering*, vol. 12, no. 1, p. 2316170, 2024.

[21] X. Bu, W. Yu, L. Cui, Z. Hou, and Z. Chen, "Event-triggered data-driven load frequency control for multiarea power systems," *IEEE Transactions on Industrial Informatics*, vol. 18, no. 9, pp. 5982–5991, 2021.